

## Polarized Crystal Absorption Spectra and Electronic States of Tetraethylammonium Hexabromodiplatinate(II)

DON S. MARTIN, Jr.,\* RHONDA M. RUSH, and TIMOTHY J. PETERS

Received May 28, 1975

AIC50364U

Polarized crystal electronic absorption spectra are reported at 300 and 15 K for normally cleaved crystals of  $[\text{N}(\text{C}_2\text{H}_5)_4]_2\text{Pt}_2\text{Br}_6$ . The spectra provide the polarization of the transitions with respect to the three molecular axes of the  $\text{Pt}_2\text{Br}_6^{2-}$  ion. The excited states have been assigned under the  $D_{2h}$  point group symmetry of the ion. There is sufficient delocalization of the d electrons that both spin-forbidden and spin-allowed  $d \leftarrow d$  transitions have strongly enhanced intensities and have dipole-allowed character in contrast to the  $\text{PtBr}_4^{2-}$  ion. Although the energies of  $d \leftarrow d$  transitions are similar for  $\text{PtBr}_4^{2-}$  and  $\text{Pt}_2\text{Br}_6^{2-}$ ,  $M \leftarrow L$  charge-transfer transitions occur at lower energies for the dimeric ion. The polarization of these intense transitions indicates that they correspond to electron transfers from terminal bromides.

### Introduction

The polarized electronic spectra for the square-planar ions of platinum(II)  $\text{PtCl}_4^{2-}$  and  $\text{PtBr}_4^{2-}$  in crystals of their potassium salts have been well characterized.<sup>1,2</sup> In these salts the spectra for isolated but oriented free ions are observed. The transition energies and intensities correlate well with the spectra of these ions in aqueous solutions. The temperature dependence of the intensities for these species indicates that the  $d \leftarrow d$  transitions, which are symmetry forbidden, occur by vibronic excitation. The distances between platinum atoms in these salts are greater than 4.1 Å.

In several compounds where the Pt-Pt distances are less than 3.5 Å, there are striking crystal effects in the spectra. For example, in the Magnus green salt,  $\text{Pt}(\text{NH}_3)_4\text{PtCl}_4$ , where the planar anions alternate in linear stacks, the shifts of  $d \leftarrow d$  transitions cause a dark green color<sup>3</sup> in contrast to the red color of  $\text{PtCl}_4^{2-}$  in  $\text{K}_2\text{PtCl}_4$  and in aqueous solution and the colorless  $\text{Pt}(\text{NH}_3)_4^{2+}$  in  $\text{Pt}(\text{NH}_3)_4\text{Cl}_2$ . There is also a large red shift for an intense transition polarized in the stacking direction (normal to the ionic plane). The forbidden transitions with this polarization which "borrow" intensity from this intense band are therefore strikingly enhanced in intensity. Similar phenomena occur in the spectra of  $\text{Pt}(\text{en})\text{Cl}_2$  and  $\text{Pt}(\text{en})\text{Br}_2$  (en is ethylenediamine) where the planar molecules stack with spacings of 3.39 and 3.50 Å, respectively. In addition, there are spectral bands which have been attributed to intermolecular electron transfers which yield ionic exciton transition states.<sup>4,5</sup>

The dimeric anion  $\text{Pt}_2\text{Br}_6^{2-}$  is especially interesting because the Pt-Pt distance is only 3.55 Å.<sup>6</sup> This distance is comparable to the Pt-Pt separations for which strong crystal effects have been observed in the spectrum of the monomeric compounds. With the two bromide bridges, each platinum atom has the square-planar arrangement of bromide ligands.

It has been possible in the present work to record single-crystal spectra over an extended wavelength range for  $[\text{N}(\text{C}_2\text{H}_5)_4]_2\text{Pt}_2\text{Br}_6$  at room temperature and in a liquid helium cryostat at 15 K. Day, Smith, and Williams<sup>7</sup> reported earlier crystal spectra for this compound over a very limited wavelength range at room temperature only.

### Experimental Section

$[\text{N}(\text{C}_2\text{H}_5)_4]_2\text{Pt}_2\text{Br}_6$  had been prepared by the method of Harris, Livingstone, and Stephenson.<sup>8</sup> The salt, recrystallized from acetone, forms thin crystal plates with a micaceous cleavage. A mass of crystals on a microscope slide were washed with 1 drop of an ethanol-water solution in which the salt is insoluble. Single crystals suitable for spectroscopy could be selected from those on the slide. These crystals were sometimes less than 5  $\mu$  thick. Such crystals with light polarized in the direction of the extinction for high refractive index (designated the high extinction polarization) were pale yellow in transmitted white light. They appeared colorless for the "low" extinction polarization. A thicker crystal grown from nitrobenzene solution appeared brown

with the high extinction and faintly pink in the low extinction. The dichroism was much stronger than for  $\text{K}_2\text{PtBr}_4$ .<sup>2</sup> The index of refraction for the low extinction,  $n^{25D}$ , was found by the Becke line method to be 1.5803. The index of refraction for the high extinction was <1.74 ( $\text{CH}_2\text{I}_2$ ) but was above the range of our refractometer. From the interference colors between crossed polarizers, the birefringence of the crystal plates was estimated to be 0.11 so the indicated index of refraction for the high extinction is 1.69.

Stephenson<sup>6</sup> reported the structure of  $[\text{N}(\text{C}_2\text{H}_5)_4]_2\text{Pt}_2\text{Br}_6$  to be triclinic  $P\bar{1}$ , with  $a = 7.60$  Å,  $b = 8.83$  Å,  $c = 12.34$  Å,  $\alpha = 105.6^\circ$ ,  $\beta = 84.0^\circ$ , and  $\gamma = 112.8^\circ$ , with one formula unit per unit cell.

A thin crystal plate was selected for which the extinction directions could be accurately measured with respect to the crystal edges. X-ray precession photographs were obtained. The crystal was mounted on an automatic four-circle diffractometer and four octants of data were collected. The real cell axes were located so the angles between the extinction directions and the real axes could be determined. The diffraction data were refined sufficiently to confirm the presence of Stephenson's structure and the platinum-bromide bond lengths. The cleavage face was identified on the diffractometer as the 001 under Stephenson's axial assignments. This result disagrees with the assignment of the cleavage face as the 100 by Day et al.,<sup>7</sup> who based their assignments on the measured angles between the crystal edges.

The techniques for measurement of crystal spectra have been described previously.<sup>9</sup> For triclinic crystals extinction directions are not fixed but can change with wavelength. Extinction directions at various wavelengths were determined from the location of the maximum absorbance recorded as the polarizer was rotated. It appears that the axes of the indicatrix ellipsoids must be nearly coincident with the axes of the  $\text{Pt}_2\text{Br}_6^{2-}$  ion in the crystal. In any event no rotation of the extinction directions for the cleavage face could be detected over the wavelength region followed, and any such rotation was no more than  $\pm 1^\circ$ .

Because of the bulky anion in the crystal and the fact that the anion contains two platinum atoms, the molar concentration of the compound in the crystal is rather low, only 2.38 M ( $\text{Pt}_2\text{Br}_6^{2-}$ ). Since such thin crystals were available, it was possible to follow absorptions up to a molar absorptivity of 4000  $\text{cm}^{-1} \text{M}^{-1}$  ( $\text{Pt}_2\text{Br}_6^{2-}$ ).

The thickness of crystals was established by the interferometric method.<sup>2,3</sup> A crystal was found with rather weak but usable interference from the multiple internal reflections. The wavelengths for six maxima and six minima were measured between 434.5 and 598.4 nm for the low extinction polarization. Methods for the calculation of crystal thickness have been further investigated since the method was utilized previously for estimating crystal thickness for  $\text{K}_2\text{PtBr}_4$  and Magnus' green salt. For an absorbance minimum there is constructive interference between transmitted light and the wave which has been internally reflected by the crystal faces. The crystal thickness  $L$ , is an integral half-number of wavelengths or

$$L = N/2\bar{\nu}_N n_N \quad (1)$$

where  $N$  is an integer,  $\bar{\nu}_N$  is the wavenumber of the absorbance minimum, and  $n_N$  is the refractive index of the crystal at  $\bar{\nu}_N$ . For successive maxima and minima therefore

$$n_m \bar{\nu}_m / n_N \bar{\nu}_N = 1 + m/N \quad (2)$$

where  $n_m$  is the index of refraction of a maximum or minimum at

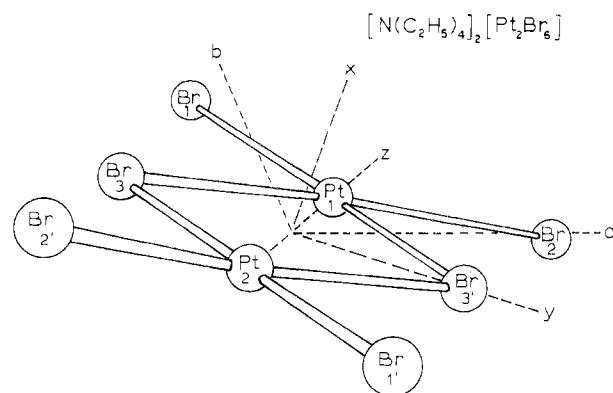


Figure 1. Orthogonal projection of the  $\text{Pt}_2\text{Br}_6^{2-}$  ion upon the 001 cleavage face.

$\bar{\nu}_m$ , and  $m$  is half-integral for maxima and integral for minima. From eq 2 can be derived the expression

$$\lim_{m \rightarrow 0} m \bar{\nu}_N / (\bar{\nu}_m - \bar{\nu}_N) = N + N(dn/d\bar{\nu})_N \bar{\nu}_N / n_N \quad (3)$$

Now the wavelengths for the maxima and minima can be determined with an uncertainty of 0.1–0.2 nm from the spectrophotometric measurements. From a linear least-squares fit of  $m \bar{\nu}_m / (\bar{\nu}_m - \bar{\nu}_N)$  vs.  $\bar{\nu}$ , a rather precise value of the limit of this quantity as  $m \rightarrow 0$  can be obtained. According to eq 3,  $\lim_{m \rightarrow 0} m \bar{\nu}_m / (\bar{\nu}_m - \bar{\nu}_N)$  serves as an approximate value of  $N$  and the last term in the equation is a correction term. However, the correction term, which includes the dispersion,  $dn/d\bar{\nu}$ , may not be negligible. For the particular crystal which exhibited the interference waves, the indicated  $\lim_{m \rightarrow 0} m \bar{\nu}_m / (\bar{\nu}_m - \bar{\nu}_N)$  was 27.83 for  $\bar{\nu}_N = 18730 \text{ cm}^{-1}$ . The maximum reasonable value for  $N$  would therefore be 27 since a larger value would indicate an unexpected negative dispersion. It has been concluded that the most probable value for  $N$  was 27 since a reasonable dispersion of  $2.6 \times 10^{-6} \text{ cm}$  would be indicated by eq 3. However, a value of 26 is not completely excluded; it would correspond to a dispersion of  $5.9 \times 10^{-6} \text{ cm}$ . However, a dispersion of nearly  $10^{-5} \text{ cm}$  which would be indicated by an  $N$  of 25 appears very unlikely from the dispersions found for a number of platinum and palladium coordination compounds. The crystal thickness was calculated to be  $4.6 \pm 0.2 \mu$  from the value of  $N = 27$  in eq 1. The thicknesses of other crystals were obtained by comparing their absorbances at suitable wavelengths with those of this crystal.

## Results and Discussion

**Crystal Spectra.** The crystal structure of Stephenson<sup>8</sup> demonstrated that the  $\text{Pt}_2\text{Br}_6^{2-}$  ion is essentially planar with  $D_{2h}$  symmetry, and the electronic states have been treated under this point group. An orthogonal projection of the  $\text{Pt}_2\text{Br}_6^{2-}$  ion upon the 001 cleavage face of the crystal is shown in Figure 1. The crystal space group however requires only the inversion center symmetry element for  $\text{Pt}_2\text{Br}_6^{2-}$ . The ring formed by the two platinum atoms and the two bridging bromides is therefore planar. The  $z$  axis for the ion was placed along the Pt–Pt direction and constitutes the long molecular axis as shown in Figure 1. The  $x$  or short molecular axis was taken normal to the ring plane, and the  $y$  or intermediate axis was then normal to these axes. This  $y$  axis passed within 0.02 Å of the sites specified by Stephenson for the  $\text{Br}_3$  and  $\text{Br}_3'$  or bridging bromides. The wave front for light transmitted through the crystal therefore passes through the  $\text{Pt}_2\text{Br}_6^{2-}$  ion nearly end on. The wave front normal and the  $z$  axis form an angle of  $16.23^\circ$ . The high extinction direction in the 001 face was  $18 \pm 1^\circ$  from the  $a$  axis and within the experimental uncertainty was coincident with the projection of the  $y$  axis on the face which was  $18.35^\circ$  from the  $a$  axis. The  $y$  axis formed an angle of only  $8.60^\circ$  with its projection on this face. The contributions to the absorption for the high extinction were therefore as follows:  $y$ , 98%;  $z$ , 2%;  $x$ ,  $\sim 0.1\%$ . The absorption for the high extinction therefore provides effectively the  $y$  transition moment. The low extinction direction on the 001

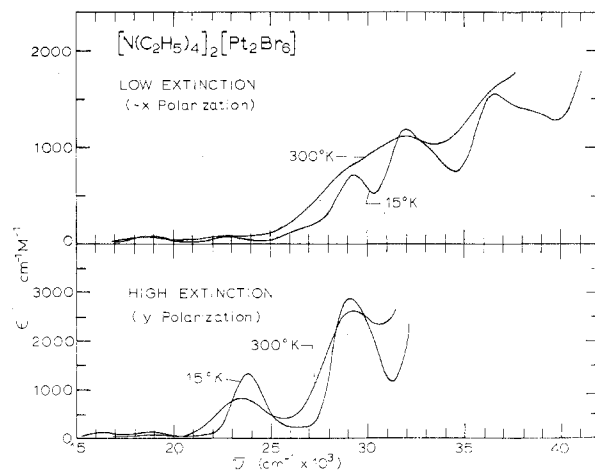


Figure 2. Polarized crystal spectra for  $[\text{N}(\text{C}_2\text{H}_5)_4]_2\text{Pt}_2\text{Br}_6$ : high extinction, crystal  $3.2 \mu$  thick; low extinction, crystal  $6.7 \mu$  thick.

face is  $13.7^\circ$  from the  $x$  axis and  $76.3^\circ$  from the  $z$  axis. Contributions to the absorption therefore are as follows:  $x$ , 94%;  $z$ , 6%;  $y$ , 0.

The spectra for the high and low extinctions are shown in Figure 2. As is visually apparent, the absorption for the high extinction is much stronger than for the low extinction at all wavelengths. For the high extinction, primarily the  $y$  polarization, two strong peaks are evident. The lower energy peak has an  $\epsilon_{\text{max}}$  of ca.  $800 \text{ cm}^{-1} \text{ M}^{-1}$  at room temperature which increases to  $1400 \text{ cm}^{-1} \text{ M}^{-1}$  at  $23900 \text{ cm}^{-1}$  at 15 K. The peak height at  $29200 \text{ cm}^{-1}$  also increases from  $3300$  to  $3700 \text{ cm}^{-1} \text{ M}^{-1}$  upon cooling to 15 K. The increase in peak height is indicative of a transition with a nonzero transition dipole. This temperature-dependent behavior is in contrast to dipole-forbidden transitions which are excited by the vibronic interaction with the odd vibrations which serve as perturbations to mix odd wave functions into the even electronic states. The high extinction spectra for this crystal are strikingly different from the spectra of  $\text{K}_2\text{PtBr}_4$ .<sup>2</sup> For that crystal the region  $24000\text{--}30000 \text{ cm}^{-1}$  is occupied by  $d \leftarrow d$  transitions which are excited exclusively by the vibronic mechanism. At 15 K the highest molar absorptivity of  $\text{K}_2\text{PtBr}_4$  is about  $70 \text{ cm}^{-1} \text{ M}^{-1}$ . Even if the  $\epsilon$ 's of  $\text{Pt}_2\text{Br}_6^{2-}$  are divided by 2 to place them on a comparable basis per platinum atom, they still remain an order of magnitude higher and seem much too intense to be attributed to crystal field asymmetries.

The striking contrast between the high and low extinction spectra attests to how well the molecular orientations isolate the  $y$  axis absorptions in the high extinction. The absorption in the low extinction polarization at  $23000 \text{ cm}^{-1}$  is less than  $30 \text{ cm}^{-1} \text{ M}^{-1}$  with no evidence of a peak. At room temperature the absorption in the low extinction polarization increases gradually from  $20000$  to  $38000 \text{ cm}^{-1}$  with little structure other than a shoulder at ca.  $32000 \text{ cm}^{-1}$ . At 15 K a number of well-resolved, moderately strong peaks have appeared in the low extinction polarization. These peaks appear to be superimposed on an absorption which increases with  $\bar{\nu}$  but which has fallen off with decreasing temperature. The band at  $29000 \text{ cm}^{-1}$  has a peak about  $300 \text{ cm}^{-1} \text{ M}^{-1}$  above the increasing absorption. Bands at  $32000$  and  $36500 \text{ cm}^{-1}$  have corresponding  $\epsilon$ 's of  $300$  and  $400 \text{ cm}^{-1} \text{ M}^{-1}$ , respectively. Weaker peaks are evident at  $26500$  and ca.  $33000 \text{ cm}^{-1}$ . It seems that at least the three stronger peaks are dipole allowed from the extent to which they have grown above the general absorption.

Spectra were also recorded for the low extinction in which a crystal was tilted or rotated in the light beam about the high extinction axis. A consequence of such a rotation is to change the angle between the  $z$  axis and the wave front normal for the light. Two spectra for positive and negative tilt angles are

Table I. Transitions Observed for  $K_2PtBr_4$  and for  $[N(C_2H_5)_4]_2Pt_2Br_6$  Crystals (Band Maxima and Molar Absorptivities for 15 K)

$K_2PtBr_4^a$				$[N(C_2H_5)_4]_2Pt_2Br_6$				
$\bar{\nu}, b \text{ cm}^{-1}$	Oscill strength $\times 10^4$		Assignment $D_{4h}$	$\nu, \text{cm}^{-1}$	Molar absorptivity, $\text{cm}^{-1} \text{M}^{-1}$	Oscill strength $\times 10^4$	Assignment $D_{2h}$	
	z polarizn	x,y polarizn						larizn
17 000	0.05	0.4		16 300	y	4	$^3A_u$ : $d_{yz} \leftarrow d_{xz}$	
19 000	1	1	$^3A_{2g} - ^3E_g$ : $\sigma^*d_{x^2-y^2} \leftarrow d_{xy}, d_{xz}, d_{yz}$	17 500	x (Vibronic)		$g \leftarrow g$	
22 700	0.2	0.9	$^3B_{1g}$ : $\sigma^*d_{x^2-y^2} \leftarrow d_{z^2}$	18 800	y	6	$^3B_{3u}$ : $d_{yz} \leftarrow d_{xy}$	
24 000		4.0	$^1A_{2g}$ : $\sigma^*d_{x^2-y^2} \leftarrow d_{xy}$	18 900	x	2	$^3B_{2u}$ : $d_{yz} \leftarrow d_{y^2-z^2}$	
27 200	4	7.0	$^1E_g$ : $\sigma^*d_{x^2-y^2} \leftarrow d_{xz}, d_{yz}$	22 300	x	2	$^3B_{2u}$ : $d_{yz} \leftarrow d_{x^2}$	
30 600	1	1	$^3E_u$ : $\sigma^*d_{x^2-y^2} \leftarrow L\pi$	23 800	y	150	$^1B_{2u}$ : $d_{yz} \leftarrow d_{y^2-z^2}$	
33 800	2		$^1B_{1g}$ : $\sigma^*d_{x^2-y^2} \leftarrow d_{z^2}$	26 500	x	10	$^1B_{3u}$ : $d_{yz} \leftarrow d_{xy}$	
34 200		300	$^3B_{1g} - ^1E_g$ : $p_z \leftarrow d_{xy}$	29 000	x	35	$^1B_{3u}$ : $d_{yz} \leftarrow L\pi_{T,x}$	
35 300	0.6		$^3B_{1u}$ : $p_z \leftarrow d_{xy}$	29 200	y	320	$^1B_{2u}$ : $d_{yz} \leftarrow d_{x^2}$ or $L\pi_T$	
37 200		1300	$^1E_g - ^3B_{1g}$ : $\sigma^*d_{x^2-y^2} \leftarrow L\pi$	31 500	z	1000	$^1B_{1u}$ : $d_{yz} \leftarrow L\pi_T$	
48 100 <sup>c</sup>		8000 <sup>c</sup>	$^1A_{2u} - ^1E_u$ : $p_z \leftarrow d_{z^2}; \sigma^* \leftarrow L\sigma$	33 000	x	7	Spin-forbidden charge transfer	
				36 560	x	46	$^1B_{3u}$ : $d_{yz} \leftarrow L\pi_{B,x}$	
				38 000	x	7	Spin-forbidden charge transfer	

<sup>a</sup> From ref 1. <sup>b</sup> Energies of peaks in z and x,y polarization for corresponding bands have been averaged and oscillator strengths rounded to one significant figure. <sup>c</sup> Polarization not indicated; from solution spectrum.

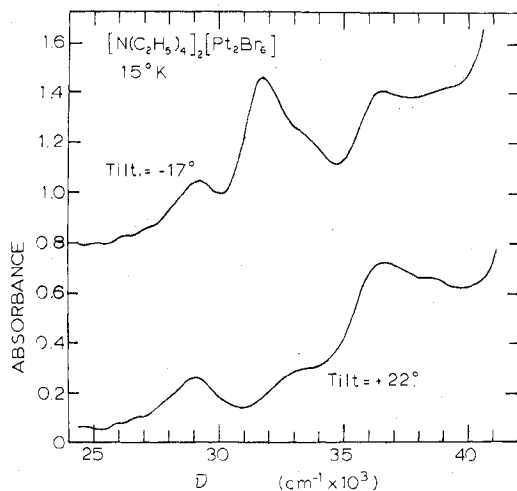


Figure 3. Low extinction spectra at 15 K which have been tilted or rotated in the light beam about the high extinction axis.

shown in Figure 3. It can be seen from the figure that at  $-17^\circ$  tilt a peak at  $31500 \text{ cm}^{-1}$  has become a dominant feature while at  $+22^\circ$  tilt it has been virtually removed from the spectrum. It is concluded therefore that the band at  $31500 \text{ cm}^{-1}$  is a strong band with z polarization with an  $\epsilon$  of at least  $9000 \text{ cm}^{-1} \text{M}^{-1}$ . A summary of the spectral data for  $[N(C_2H_5)_4]_2Pt_2Br_6$  is presented in Table I. Also, listed in Table I are the transitions of  $K_2PtBr_4$  for comparison with those of the dimer salt.

Spectra for a thick crystal in the low-energy region are shown in Figure 4. This is the spin-forbidden  $d \leftarrow d$  region for  $K_2PtBr_4$ . The room-temperature spectra in Figure 4 are in good agreement with those of Day et al.<sup>6</sup> In the low-temperature spectra bands at  $16300$  and  $18800 \text{ cm}^{-1}$  appear dipole allowed in the high extinction polarization. For the low extinction there are dipole-allowed transitions at  $18900$  and  $21700 \text{ cm}^{-1}$ . However, the temperature dependence in the region of  $17500 \text{ cm}^{-1}$  indicates the presence of a vibronically excited band.

**Electronic States Excited by  $d \leftarrow d$  Transitions.** If the two platinum atoms were essentially isolated and noninteracting, each would possess a set of d orbitals ordered as in the square-planar  $D_{4h}$  ion. These orbitals with the present choice of axes in order of increasing energy would be  $d_{x^2}$ ,  $d_{xz,xy}$ ,  $d_{y^2-z^2}$ ,

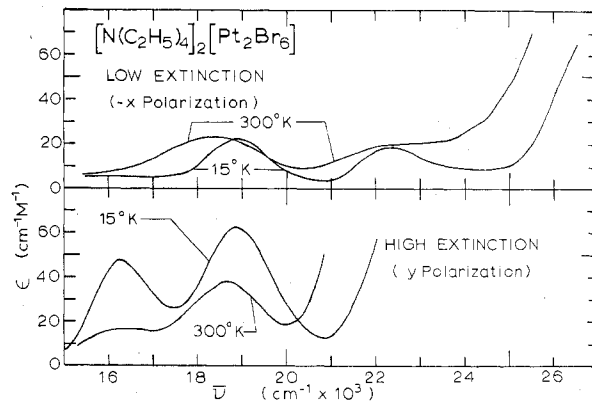


Figure 4. Polarized crystal spectra for a thick crystal ( $77 \mu$ ) of  $[N(C_2H_5)_4]_2Pt_2Br_6$ .

and  $d_{yz}$ . The last orbital represents essentially a  $\sigma$  antibonding orbital. In such a case the energies and intensities for the transition would be expected to resemble those of  $PtBr_4^{2-}$ . This behavior was not observed.

In the opposite extreme the electrons might be considered to be delocalized in molecular orbitals formed from linear combinations of equivalent orbitals. The two lowest unfilled orbitals would consist primarily of  $(d_{yz,1} + d_{yz,2})/2^{1/2}$  with  $b_{3g}$  symmetry and  $(d_{yz,1} - d_{yz,2})/2^{1/2}$  with  $b_{2u}$  symmetry under the  $D_{2h}$  group. These linear combinations participate with ligand p orbitals to comprise a pair of antibonding orbitals. The linear combinations corresponding to these two MO's have been sketched in Figure 5. The two highest filled orbitals include linear combinations of  $d_{y^2-z^2}$  orbitals with  $b_{1u}$  and  $a_g$  symmetry which are also sketched in Figure 5 together with interacting linear combinations of the ligand p orbitals. Thus, for each  $d \leftarrow d$  transition of monomeric ions there will be four transitions for the dimer. In addition, two of the four will be  $u \leftarrow g$  and may therefore be dipole allowed. Since the ground state is  $^1A_g$ , the states attained by dipole-allowed transitions with the indicated polarizations are  $B_{1u}(z)$ ,  $B_{2u}(y)$ , and  $B_{3u}(x)$ . The two ungerade states based on  $d_{yz} \leftarrow d_{y^2-z^2}$  are both  $B_{2u}$ , and the transitions to them are therefore polarized in the y direction. The symmetry of the LCAO's based on each of the d orbitals is shown in Figure 5. In addition, the symmetries of the singlet excited states are indicated together with the polarization for the dipole-allowed transitions. When possible

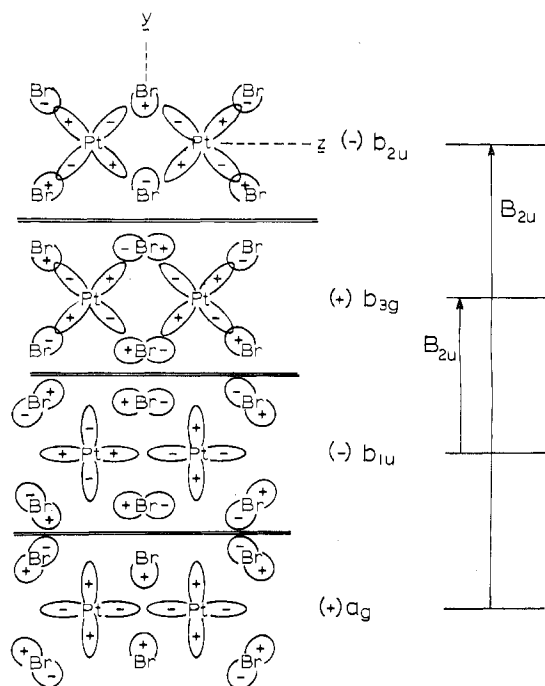


Figure 5. MO's based on LCAO's of the  $d_{yz}$  and  $d_{y^2-z^2}$  orbitals of the platinum and for bromide p orbitals with the corresponding symmetry. On the right are the dipole-allowed  $d \leftarrow d$  transitions between these orbitals.

vibrations for the  $\text{Pt}_2\text{Br}_6^{2-}$  ion are considered, transitions from each set of d orbitals into the  $\sigma^*$ 's are vibronically allowed in each polarization. It is seen from Figure 6 that orbitals based on  $d_{y^2-z^2}$  and  $d_{x^2}$  have the same symmetry and presumably may be mixed somewhat. There should be two pairs of states excited with y polarization. From the set of degenerate orbitals for the monomeric ion there will be four ungerade excited states. However, two of these are  ${}^1A_u$ , and hence transitions to them are forbidden. There will be two  ${}^1B_{3u}$  states for the  $d_{yz} \leftarrow d_{xy}$  transitions with polarization in the x direction. There should be no dipole-allowed, spin-allowed  $d \leftarrow d$  transitions with z polarization.

The separation of the pair of orbitals in the dimer, based on a single monomer orbital, will be dependent upon the overlap in the LCAO's. Accordingly, the separation of transitions for the dimer arising from a single monomer transition, as well as the intensity of the allowed transition, will be strongly dependent upon this overlap which provides the electron delocalization. A considerable part of the orbital overlap might well involve the bridging ligand p orbitals.

As the overlap between orbitals decreases, the system would approach still a third model, intermediate between the two previous extremes, in which the two platinum atoms are considered as coupled chromophores. There would be zero overlap of orbitals between the chromophores. The coupling would occur by the electrostatic forces to which are attributed the "crystal effects" upon molecular spectra. In accordance with the treatment which follows, that is utilized for crystal exciton phenomena,<sup>10</sup> the ground-state molecular wave function would be

$$\Phi^0 = \varphi_1^0 \varphi_2^0 \quad (4)$$

where  $\varphi_1^0$  and  $\varphi_2^0$  are the ground-state wave functions for the individual platinum chromophores. An excitation of  $\text{Pt}_1$  and  $\text{Pt}_2$  would be described by the functions  $\phi_1'$  and  $\phi_2'$ , respectively

$$\phi_1' = \varphi_1' \varphi_2^0; \quad \phi_2' = \varphi_1^0 \varphi_2' \quad (5)$$

where  $\varphi_1'$  corresponds to an excited state for  $\text{Pt}_1$  as, for ex-

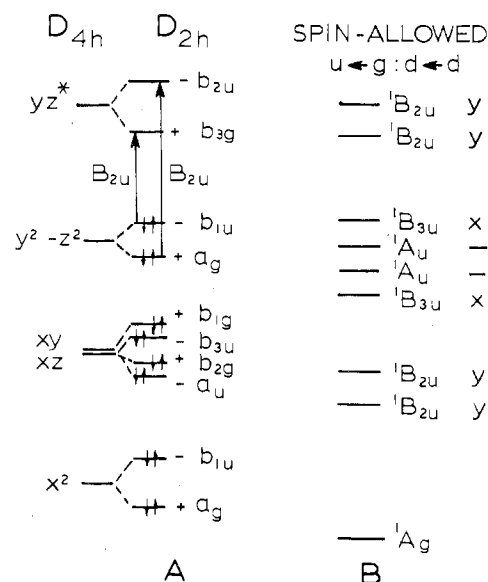


Figure 6. A. Symmetry of the LCAO's in  $\text{Pt}_2\text{Br}_6^{2-}$ , point group  $D_{2h}$ , formed from the Pt 5d orbitals under the  $D_{4h}$  point group. B. Symmetry for the spin-allowed  $u \leftarrow g$ ,  $d \leftarrow d$  states under  $D_{2h}$  and polarization of the dipole-allowed transitions.

ample,  $d_{yz,1} \leftarrow d_{y^2-z^2,1}$ , etc. There will be two molecular wave functions based on each transition

$$\Phi_+ = (\phi_1 + \phi_2)/2^{1/2} \quad (6a)$$

and

$$\Phi_- = (\phi_1 - \phi_2)/2^{1/2} \quad (6b)$$

For  $d \leftarrow d$  transitions, the  $\varphi_1' \leftarrow \varphi_1^0$  are forbidden under a static electronic transition dipole. The dipole-dipole interaction between chromophores does not provide an enhancement of the transition intensities. A significant increase in the  $d \leftarrow d$  transitions under this model must be due to the mixing in of dipole-allowed transitions by the electric field at the local sites. At the center of a platinum ion the molecular field will possess  $C_{2v}$  site symmetry. According to perturbation theory

$$\varphi_1' = \varphi_1' (d \leftarrow d) + a\varphi_1'' \quad (7)$$

where

$$a = (\int \varphi_1' (d \leftarrow d) |V_1(C_{2v})| \varphi_1'' d\tau) / (E' - E'') \quad (8)$$

and where the transition  $\varphi_1'' \leftarrow \varphi_1^0$  is dipole allowed.

As a consequence of the perturbation, the transition from the ground state to either  $\Phi_+$  or  $\Phi_-$  arising from a  $d \leftarrow d$  transition may become allowed by a static transition dipole. However, because of the inversion center, if the transition  $\Phi_+ \leftarrow \Phi^0$  is allowed by a static electric dipole, the transition  $\Phi_- \leftarrow \Phi^0$  will be forbidden and vice versa. Under the  $C_{2v}$  symmetry the  $d \leftarrow d$  transitions will be from a ground state  ${}^1A_1$  to  ${}^1B_2$ ,  $d_{yz} \leftarrow d_{y^2-z^2}$  (y polarization);  ${}^1B_1$ ,  $d_{yz} \leftarrow d_{xy}$  (x polarization);  ${}^1A_2$ ,  $d_{yz} \leftarrow d_{xz}$  (forbidden);  $B_2$ ,  $d_{yz} \leftarrow d_{x^2}$  (y polarization). Thus, this model provides the same polarization for static dipole-allowed  $d \leftarrow d$  transitions as the electron-delocalized MO model with the difference that there will be only one transition corresponding to each  $d \leftarrow d$  state rather than the two. It would appear, however, that the coupled chromophore model would be inappropriate for charge-transfer transitions where an electron from a bridging ligand might be transferred to an orbital on either platinum.

In the spectral region where only spin-allowed  $d \leftarrow d$  transitions are observed for  $\text{K}_2\text{PtBr}_4$ , there are two intense bands occurring for  $\text{Pt}_2\text{Br}_6^{2-}$  with y polarization. These occur

at 23800 and 29200  $\text{cm}^{-1}$ . The two transitions in  $\text{PtBr}_4^{2-}$ , which lead to  $x, y$ -allowed transitions, are at 24000  $\text{cm}^{-1}$  and 33800  $\text{cm}^{-1}$ . There is a close energy match between the lower such transition for  $\text{PtBr}_4^{2-}$  and  $\text{Pt}_2\text{Br}_6^{2-}$ . It must be decided therefore whether or not the transition at 29200  $\text{cm}^{-1}$  of  $\text{Pt}_2\text{Br}_6^{2-}$  corresponds to the other transition, arising from  $d_{yz} \leftarrow d_{y^2-z^2}$ . In this consideration it was noted that the strong band in  $z$  polarization 31500  $\text{cm}^{-1}$  must certainly not be a  $d \leftarrow d$  transition but rather a ligand to metal charge transfer. It will be shown below that there must be two such transitions, one to each of the orbitals based on the  $\sigma^*(d_{yz})$  orbitals. Since only one strong transition is seen over the entire energy range, it has been concluded that any splitting of the orbital energies is so small that splitting of the transition is not resolved under the spectral bands. With this regard the coupled chromophore model appears the most satisfactory. However the band at 23800  $\text{cm}^{-1}$  appears to have 10% of the intensity of a fully allowed charge-transfer transition. Such a large intensity borrowing, due to the site symmetry, appears somewhat unrealistic. For example, when chloride is replaced by  $\text{NH}_3$  in  $\text{Pt}(\text{NH}_3)\text{Cl}_3^-$ , the corresponding transition is considerably weaker.<sup>11</sup> It appears therefore that orbital overlap and electron delocalization may be needed to account for the intensities, even though it is not enough to effect a sufficiently large splitting of the transition energies under the fairly broad bands.

Accordingly, the band at 23800  $\text{cm}^{-1}$  in  $y$  polarization has been assigned as  ${}^1\text{B}_{2u} \leftarrow {}^1\text{A}_g$  ( $d_{yz} \leftarrow d_{y^2-z^2}$ ). Its intensity is 37 times greater than the corresponding transition in  $\text{K}_2\text{PtBr}_4$  at 24000  $\text{cm}^{-1}$ . The two  $d_{y^2-z^2}$  orbitals are  $\sigma$  and  $\sigma^*$  in character about the  $z$  axis and the  $d_{yz} \leftarrow d_{y^2-z^2}$  transitions under the molecular orbital model can be considered as  $\pi_z \leftarrow \sigma_z$  about that axis.

The band at 29200  $\text{cm}^{-1}$  is considerably more intense than the one at 23800  $\text{cm}^{-1}$ . There is a possibility that it corresponds to  ${}^1\text{B}_{2u} \leftarrow {}^1\text{A}_g$  arising from  $d_{yz} \leftarrow d_{xz}$ . At this energy the absorption in  $\text{K}_2\text{PtBr}_4$  is quite low. If this is the correct band assignment, then it occurs 4300  $\text{cm}^{-1}$  below the corresponding assigned transition at 33800  $\text{cm}^{-1}$  in  $\text{K}_2\text{PtBr}_4$ . The other assigned  $d \leftarrow d$  transitions match the  $\text{K}_2\text{PtBr}_4$  energies rather closely. However, that 33800- $\text{cm}^{-1}$  transition is much weaker than the other  $d \leftarrow d$  transitions, and its assignment must be considered as rather uncertain. An alternative assignment for the 29200- $\text{cm}^{-1}$  band in the dimer is to a  $\text{Pt} \leftarrow \text{Br}$  charge transfer. This possibility will be discussed further in the consideration of the charge-transfer states.

For the  $x$  polarization in Figure 2, there is a shoulder at 26500  $\text{cm}^{-1}$  which is rather weak with an  $\epsilon$  of about 100  $\text{cm}^{-1} \text{M}^{-1}$ . This band has been assigned as the  ${}^1\text{B}_{3u} \leftarrow {}^1\text{A}_g$  ( $d_{yz} \leftarrow d_{xy}$ ) transition(s). The energy is close to that of the  ${}^1\text{E}_g \leftarrow {}^1\text{A}_{1g}$  transition of  $\text{K}_2\text{PtBr}_4$ . Under the coupled-chromophore model this band obtains its intensity by the mixing in of higher allowed transitions with  $x$  polarization. Since all transitions up to 42000  $\text{cm}^{-1}$  are rather weak, the low intensity in this band in contrast to the one at 23800  $\text{cm}^{-1}$  in  $y$  polarization might be expected. The molecular orbital model would also provide a low intensity since the electron transfer for such a transition would be from an orbital with  $\delta_z$  symmetry, concentrated in a plane normal to the  $z$  axis, into an orbital with  $\pi_x$  symmetry. The decrease in the overall intensity throughout this energy region as the temperature decreases for the  $x$ -polarized spectrum is consistent with the presence of a number of vibronically allowed transitions.

**Spin-Forbidden  $d \leftarrow d$  Transitions.** To determine selection rules for spin-forbidden transitions, the electronic wave functions, including spin, must be considered in the double rotational point group,  $D_2'$ . In this group the singlet spin function is  $A'$  and the triplet functions are  $B_1'$ ,  $B_2'$ , and  $B_3'$ . As a consequence of spin-orbit coupling, if the transition to

Table II. Symmetry under the  $D_{2h}$  Group for the LCAO's Formed by the Bromide p Orbitals<sup>a</sup>

Bromide type	Orbital type	Symmetry	
		LCAO	Singlet ungerade excited states (polarizn)
Terminal	$\pi_{T,x}$	$b_{1g}, b_{2g}, a_u, b_{3u}$	$2 {}^1\text{A}_u, 2 {}^1\text{B}_{3u} (x)$
	$\pi_{T,h}$	$a_g, b_{3g}, b_{1u}, b_{2u}$	$2 {}^1\text{B}_{1u} (z), 2 {}^1\text{B}_{2u} (y)$
	$\sigma_T$	$a_g, b_{3g}, b_{1u}, b_{2u}$	$2 {}^1\text{B}_{1u} (z), 2 {}^1\text{B}_{2u} (y)$
Bridging	$\pi_{B,x}$	$b_{3u}, b_{1g}$	${}^1\text{A}_u, {}^1\text{B}_{3u} (x)$
	$\text{p}_{B,y}$	$a_g, b_{2u}$	${}^1\text{B}_{1u} (z), {}^1\text{B}_{2u} (y)$
	$\text{p}_{B,z}$	$b_{3g}, b_{1u}$	${}^1\text{B}_{1u} (z), {}^1\text{B}_{2u} (y)$

<sup>a</sup> Symmetry of the  $M \leftarrow L$  electron-transfer states with the indicated polarization of dipole-allowed transitions.

a singlet state (in  $D_{2h}$ ) is dipole allowed in one polarization,  $x, y,$  or  $z$ , there will be transitions to two primarily triplet states which will be dipole allowed in the other polarizations. Such transitions will be weak in comparison to the dipole-allowed spin-allowed transitions. The transition to the third triplet state will be dipole forbidden but vibronically allowed. A transition to the  ${}^3\text{A}_u$  states will be dipole allowed in each of the three polarizations. Since the spin-orbit perturbation mixes in stronger transitions in  $y$  than in  $x$  polarizations, the  $y$ -polarization spin-forbidden bands are the more intense and indeed exceed the spin-allowed  $d \leftarrow d$  transitions of  $\text{K}_2\text{PtBr}_4$  in intensity. Since the  ${}^3\text{B}_{2u}$  transitions are dipole forbidden in  $y$  polarization, the two transitions at 16300 and 18800  $\text{cm}^{-1}$  for which the temperature dependence indicates dipole-allowed character are presumably components of  ${}^3\text{B}_{3u}$  and  ${}^3\text{A}_u \leftarrow {}^1\text{A}_g$ ,  $d_{yz} \leftarrow d_{xy}$  and  $d_{xz}$ . For the  $x$  polarization, since the  ${}^1\text{B}_{2u}$  transition falls at 23800  $\text{cm}^{-1}$ , the  ${}^3\text{B}_{2u}$  transition must be associated with the lower energy or 18900- $\text{cm}^{-1}$  dipole-allowed band. The band at 22300  $\text{cm}^{-1}$  may be a  ${}^3\text{B}_{2u}$  transition which is associated with the singlet at 29200  $\text{cm}^{-1}$ . The absorption in the vicinity of 17500  $\text{cm}^{-1}$  which seems to be dipole forbidden but vibronically allowed may be a component of the transition arising from one of the  $g \leftarrow g$  transitions. The assignments of the spin-forbidden states is, of course, rather speculative and there may be considerable mixing of the states as well.

**Ligand to Metal Charge-Transfer Transitions.** Some  $M \leftarrow L$  charge-transfer transitions are dipole allowed and should occur at high energies. For  $\text{Pt}_2\text{Br}_6^{2-}$  there are terminal and bridging bromide ligands which must be considered separately. The charge-transfer transitions involve an electron transfer from essentially a bromide p orbital into one of the two  $\sigma^*$  orbitals based on the  $d_{yz}$ 's. The  $x, y,$  and  $z$  axes on each ligand have been taken parallel to the corresponding molecular axes. It is convenient to take linear combinations of the  $p_z$  and  $p_y$  orbitals of the terminal bromides to construct  $\sigma_T$  and in-plane  $\pi_{T,h}$  orbitals. The  $p_x$  orbitals constitute out-of-plane  $\pi_{T,x}$  orbitals. The irreducible representations for the 12 symmetry-adapted LCAO's arising from these orbitals on the terminal bromides are presented in Table II. The linear combinations of  $\sigma_T$  and  $\pi_{T,h}$  orbitals serve as functions for identical sets of irreducible representations. However, the difference between the energy of the  $\sigma$  and  $\pi$  bonds is expected to provide an energy separation between the two types. For  $\text{PtBr}_4^{2-}$  the separation between the allowed  $\sigma^* \leftarrow L\pi$  and the  $\sigma^* \leftarrow L\sigma$  transitions appears to be at least 11000  $\text{cm}^{-1}$ . The LCAO's for the  $\pi_{T,x}$  are of pure  $\pi$  character however. Also presented in Table II are the symmetries for possible singlet, ungerade excited states for electron transfer from each of the molecular orbitals.

For the bridging bromides the  $\text{p}_{B,y}$  and  $\text{p}_{B,z}$  orbitals cannot be combined into  $\sigma$  and  $\pi$  type orbitals. In fact, all four of the LCAO's from these are strongly involved in the  $\text{Pt}-\text{Br}$   $\sigma$  bonds. The  $\text{p}_{B,x}$  orbitals on the other hand provide LCAO's which have pure out-of-plane  $\pi$  character. The symmetry for

the LCAO's of the bridging bromide p orbitals and of the singlet ungerade states are also included in Table II.

In assigning the transitions it is profitable to compare the charge-transfer spectra with those of the monomeric ions.  $\text{PtBr}_4^{2-}$  has an intense band at  $37000\text{ cm}^{-1}$  which can be assigned to  $\sigma^* \leftarrow L\pi$ . The next strong band at higher energy is at  $48000\text{ cm}^{-1}$ . There is a question as to whether this band corresponds to  $\sigma^* \leftarrow L\sigma$  or  $p \leftarrow d$ . However, the  $\sigma^* \leftarrow L\sigma$  states cannot lie below this energy. The crystal spectra indicate that for  $\text{K}_2\text{PtBr}_4$  the intense  $\sigma^* \leftarrow L\pi$  transitions correspond to electron transfers from in-plane  $\pi$  orbitals.<sup>2</sup> Presumably, this intensity results from some mixing of  $\sigma$  and  $\pi$  orbitals. Any dipole-allowed  $\sigma^* \leftarrow L\pi$  transition from an out-of-plane  $L\pi$  orbital in the vicinity of  $37000\text{ cm}^{-1}$  is very weak with an  $\epsilon$  of not over  $1000\text{ cm}^{-1}\text{ M}^{-1}$ . Similar results<sup>12</sup> have been obtained for  $\text{PdCl}_4^{2-}$  and  $\text{PdBr}_4^{2-}$ . The present work appears consistent with such conclusions because the low absorption in the  $x$  polarization permits this spectrum to be recorded to  $41000\text{ cm}^{-1}$ . All of the dipole-allowed transitions for the  $x$  polarization arise from electron transfers from the out-of-plane  $p_x$  orbitals on the bromides.

Mason and Gray<sup>13</sup> have measured spectra for salts of dimeric palladium(II) ions in glasses at 77 K. They noted that intense transitions occurred in the vicinity of the  $\sigma^* \leftarrow L\pi$  and  $\sigma^* \leftarrow L\sigma$  transition energies for the corresponding monomeric ions. In addition, there were intense transitions at lower energies than either of these. The intense band at  $31500\text{ cm}^{-1}$  in  $z$  polarization of  $\text{Pt}_2\text{Br}_6^{2-}$  confirms a similar behavior for  $\text{Pt}_2\text{Br}_6^{2-}$ . This is the only strong band in  $z$  polarization up to an energy of  $42000\text{ cm}^{-1}$ . Since it presumably must correspond to an electron transfer from a ligand  $\pi$  orbital, this band is assigned to the pair of transitions to  ${}^1\text{B}_{1u}$  states excited by  $\sigma^* \leftarrow \pi_{T,h}$ .

Such an assignment of a  $\sigma^* \leftarrow \pi_{T,h}$  band at such a low energy suggests that the band at  $29400\text{ cm}^{-1}$  in  $y$  polarization may also have a similar origin; i.e., it might be largely the transitions to the pair of  ${}^1\text{B}_{2u}$  states arising from the  $\sigma^* \leftarrow \pi_{T,h}$ . However, as indicated above, there does appear to be further strong absorption in  $y$  polarization no higher than  $37000\text{ cm}^{-1}$ . Hence, there may be a mixing of  $d \leftarrow d$  and  $\sigma^* \leftarrow L\pi$  character in two strong bands with  $y$  polarization at  $29400$  and at about  $35000\text{--}37000\text{ cm}^{-1}$ .

For  $x$  polarization the two bands at  $29000$  and  $36500\text{ cm}^{-1}$  have been assigned as electron transfers from the  $\pi_{T,x}$  and  $\pi_{B,x}$  to  $\sigma^*$ 's. Since the charge transfer in  $z$  polarization occurred at such a low energy and was necessarily an electron transfer from  $\pi_T$  orbitals, the  ${}^1\text{B}_{3u}$  band at the lower energy is probably also a charge transfer from the terminal bromides.

The bridging bromide, in bonding to two platinum, donates a greater total electronic charge to platinum. Each platinum in turn receives less electronic charge from a bridging ligand than from a terminal ligand. Both bridging ligands and platinum, therefore, are more positive than in the monomeric ions. Such a charge redistribution appears consistent with the  $M\sigma^* \leftarrow L\pi_B$  transition having nearly the same energy as the  $M \leftarrow L\pi$  charge-transfer bands of the monomer and the  $M\sigma^* \leftarrow L\pi_T$  having lower energies. There do appear to be quite weak bands at  $33000$  and  $39000\text{ cm}^{-1}$ . These transitions may very likely be spin-forbidden bands of the charge transfers.

The molecular orientation and crystal optics for  $[\text{N}(\text{C}_2\text{H}_5)_4]_2\text{Pt}_2\text{Br}_6$  have proved to be exceedingly and perhaps unexpectedly favorable for polarized crystal spectroscopy. Thus, even though the crystal possesses a triclinic structure, it has been possible to characterize the absorption bands polarized along two of the molecular axes of  $\text{Pt}_2\text{Br}_6^{2-}$  over an extensive energy region. In addition, one strong band can be identified for the third molecular axis. A strong ligand field of low symmetry, can, of course, compromise the selection rules

for molecular polarization. However, the purity of the bands in the various polarizations indicates that such crystal fields are not an important influence for the observed transitions in this crystal.

Although the splitting of transitions as a consequence of orbital overlap and electron delocalization cannot be observed in the spectra of this salt, it is believed to contribute to the intensity of the dipole-allowed  $d \leftarrow d$  transitions. For one thing the Pt-Pt distance of  $3.55\text{ \AA}$  is only  $0.05\text{ \AA}$  longer in  $\text{Pt}_2\text{Br}_6^{2-}$  than in  $\text{Pt}(\text{en})\text{Br}_2$  where an intermolecular  $d \leftarrow d$  electron transfer transition was observed.<sup>5</sup> Indeed the  ${}^1\text{B}_{2u} \leftarrow {}^1\text{A}_g$  band for  $\text{Pt}_2\text{Br}_6^{2-}$  was more intense than the intermolecular electron-transfer transition in  $\text{Pt}(\text{en})\text{Br}_2$ . However, for the latter the transition is  $\delta \leftarrow \pi$  with respect to the Pt-Pt axis whereas for  $\text{Pt}_2\text{Br}_6^{2-}$  the  ${}^1\text{B}_{2u} \leftarrow {}^1\text{A}_g$  transition is  $\pi_z \leftarrow \sigma_z$  with respect to this axis.  ${}^1\text{B}_{1u} \leftarrow {}^1\text{A}_g$ , which is also  $\pi_z \leftarrow \delta_z$ , on the other hand matched rather closely the intensity of the intermolecular electron transfer of  $\text{Pt}(\text{en})\text{Br}_2$  oscillator strength ( $14 \times 10^{-4}$  at 15 K). In addition we have recently learned in a communication from Gray and coworkers<sup>14</sup> that they have obtained crystal spectra for bis[1,2,3-tris(dimethylamino)-cyclopropenium] hexachlorodiplatinate(II) with the  $\text{Pt}_2\text{Cl}_6^{2-}$  ion. For that system they also observed enhanced intensities for the  $d \leftarrow d$  transitions but, in addition, resolved two bands in  $y$  polarization, separated by  $1650\text{ cm}^{-1}$  which would be assigned as  ${}^1\text{B}_{2u} \leftarrow {}^1\text{A}_g$  ( $d_{yz} \leftarrow d_{y^2-z^2}$ ). In that case the smaller Pt-Pt separation of  $3.42\text{ \AA}$  apparently provided a larger separation of bands.

Vibrational structure was observed at 15 K in bands at  $22700$  and  $24400\text{ cm}^{-1}$  for  $\text{K}_2\text{PtBr}_4$ . Such vibrational structure was completely absent for  $\text{Pt}_2\text{Br}_6^{2-}$ , which is, however, not surprising. The vibrational structure in the electronic transition arises from the Franck-Condon effect in the excitation of totally symmetric vibrations in the excited electronic states.  $\text{PtBr}_4^{2-}$  possesses only one totally symmetric ( $A_{1g}$ ) vibration whereas  $\text{Pt}_2\text{Br}_6^{2-}$  possesses four  $A_g$  vibrations. In addition, there is the doubling of the electronic transitions. Hence, each band would contain eight different progressions and their resolution might well be lost.

A component in the aqueous spectrum of  $\text{PtBr}_4^{2-}$  was reported at  $31500\text{ cm}^{-1}$  ( $\epsilon\ 600\text{ cm}^{-1}\text{ M}^{-1}$ ). This component was not observed in the crystal spectra of  $\text{K}_2\text{PtBr}_4$ , and, therefore, the component was not assigned to the  $\text{PtBr}_4^{2-}$  species in solution. This absorption coincides with the  ${}^1\text{B}_{1u} \leftarrow {}^1\text{A}_g$  ( $\epsilon\ \sim 9000\text{ cm}^{-1}\text{ M}^{-1}$ ) transition observed in the  $\text{Pt}_2\text{Br}_6^{2-}$  crystal spectra. Quite possibly, the  $31500\text{-cm}^{-1}$  component observed for  $\text{PtBr}_4^{2-}$  was due to the presence of a small amount of  $\text{Pt}_2\text{Br}_6^{2-}$  in equilibrium with the monomeric ions.

The dimeric ions formed by palladium and platinum typically have intense transitions which occur  $5000\text{--}7000\text{ cm}^{-1}$  below the intense transitions of the corresponding monomeric species. Mason and Gray<sup>13</sup> have speculated that these transitions arise from the transfer of nonbonding  $\pi$  electrons from the bridging bromide ligands to the platinum. However, the symmetry requirements from the crystal spectra clearly imply that there must be electron transfers from the terminal bromide.

Registry No.  $[\text{N}(\text{C}_2\text{H}_5)_4]_2\text{Pt}_2\text{Br}_6$ , 18475-81-5.

## References and Notes

- (1) D. S. Martin, Jr., M. A. Tucker, and A. J. Kassman, *Inorg. Chem.*, **4**, 1682 (1965).
- (2) R. F. Kroening, R. M. Rush, D. S. Martin, Jr., and J. C. Clardy, *Inorg. Chem.*, **13**, 1366 (1974).
- (3) D. S. Martin, Jr., R. M. Rush, R. F. Kroening, and P. E. Fanwick, *Inorg. Chem.*, **12**, 301 (1973).
- (4) D. S. Martin, Jr., L. D. Hunter, R. Kroening, and R. F. Coley, *J. Am. Chem. Soc.*, **93**, 5433 (1971).
- (5) R. F. Kroening, L. D. Hunter, R. M. Rush, J. C. Clardy, and D. S. Martin, Jr., *J. Phys. Chem.*, **77**, 3077 (1973).
- (6) N. C. Stephenson, *Acta Crystallogr.*, **17**, 587 (1964).

- (7) P. Day, M. J. Smith, and R. J. P. Williams, *J. Chem. Soc. A*, 668 (1968).  
 (8) C. M. Harris, S. E. M. Livingstone, and N. C. Stephenson, *J. Chem. Soc.*, 3697 (1958).  
 (9) D. S. Martin, Jr., *Inorg. Chim. Acta, Rev.*, 5, 107 (1971).  
 (10) D. P. Craig and S. H. Walmsley, "Excitons in Molecular Crystals", W. A. Benjamin, New York, N.Y., 1968.  
 (11) P. E. Fanwick and D. S. Martin, Jr., *Inorg. Chem.*, 12, 24 (1973).  
 (12) R. M. Rush, D. S. Martin, Jr., and R. G. LaGrand, *Inorg. Chem.*, 14, 2543 (1975).  
 (13) W. R. Mason, III, and H. B. Gray, *J. Am. Chem. Soc.*, 90, 5722 (1968).  
 (14) C. D. Cowman, J. C. Thibeault, R. F. Ziolo, and H. B. Gray, submitted for publication.

Contribution No. 3536 from the Department of Chemistry,  
 University of California, Los Angeles, California 90024

## Spectroscopic Studies of Perpendicular Nitrile-Metal Interactions

JAMES E. SUTTON<sup>1a</sup> and JEFFREY I. ZINK<sup>\*1b</sup>

Received September 23, 1975

AIC50703J

Metal complexes of the ligand 8-cyanoquinoline of the forms  $[M(8\text{-cyanoquinoline})_2X_2]$  ( $M = \text{Pd(II), Pt(II), Cu(II)}$ ;  $X^- = \text{Cl}^-, \text{Br}^-$ ) and  $[M(8\text{-cyanoquinoline})_2X]$  ( $M = \text{Ag(I)}$ ,  $X^- = \text{NO}_3^-$ ) have been prepared. Upon coordination, the 8-cyanoquinoline shows small shifts to lower energy in the nitrile stretching frequency which are attributed to perpendicular nitrile-metal interactions. The effects on the metal orbitals of the perpendicular interactions are studied using uv-visible and ESR spectroscopy. Red shifts in the electronic absorption spectra and increases in the  $g_{\parallel}$  values are found in the 8-cyanoquinoline complexes in comparison with the corresponding quinoline complexes. A molecular orbital description of the perpendicular nitrile-metal interactions is developed.

### Introduction

Nitriles generally utilize the lone pair of electrons on the nitrogen to form linear  $M-N\equiv C-R$  bonds in transition metal coordination complexes. However, a small number of perpendicular nitrile-metal interactions have recently been reported<sup>2-8</sup> (and in part questioned).<sup>9,10</sup> Perpendicular nitrile-metal interactions shift the nitrile stretching frequency to lower energy in contrast to linear interactions which generally result in a shift to higher energy.<sup>11</sup> The reported compounds include *o*-cyanodiphenylphosphine-manganese(I) and -rhenium(I) complexes,<sup>8</sup> cyanamide-nickel(0) complexes,<sup>2</sup> dinitrile-manganese(I) complexes,<sup>3,4</sup> and aminoacetonitrile complexes of group 4 elements<sup>6</sup> showing shifts to lower energy in the nitrile stretching frequency of about 200, 200, 190, and 70  $\text{cm}^{-1}$ , respectively. A platinum(II) complex believed to involve perpendicularly coordinated acetonitrile was reported<sup>12</sup> but was later shown to have an amidine linkage to the metal.<sup>13</sup> In most cases, spectroscopic studies of the perpendicular interaction have been restricted to ir or Raman measurements of the nitrile stretching frequency shifts.

In this study, we report the syntheses and spectroscopic studies of perpendicular nitrile-metal interactions in "classical" coordination complexes of Pd(II), Pt(II), Cu(II), and Ag(I) with 8-cyanoquinoline (Figure 1). The geometrical properties of the rigid ligand 8-cyanoquinoline are used to position the nitrile group perpendicular to a metal coordinated to the ring nitrogen (Figure 1). This ligand allows the perpendicular nitrile-metal interaction to be studied in complexes where a nitrile is ordinarily linearly coordinated.

### Experimental Section

**Materials. 8-Cyanoquinoline.** The ligand was prepared using a previously reported sealed-tube reaction<sup>14</sup> with the following modifications. After the reaction mixture from the sealed tube was extracted with benzene-ether-aqueous ammonium hydroxide, all volatile liquids in the organic layer were removed on a rotoevaporator. The pyridine was removed at room temperature under vacuum using a cold trap to collect the vaporized solvent. The remaining liquid was stirred with hexane resulting in formation of a solid which was collected and redissolved in ether. The crude product was precipitated from the ether solution with the addition of hexane, and the final product was recrystallized from ether-hexane: mp 81.5-82.5 °C;<sup>15</sup> ir peaks (in  $\text{cm}^{-1}$ ) 1609 (m), 1592 (s), 1569 (m), 1491 (s), 1466 (w), 1416 (w), 1383 (s);<sup>16</sup> <sup>13</sup>C NMR shifts  $\tau$ -151.97, -136.02, -135.02, -132.42, -125.44, -122.35.<sup>17</sup> Anal. Calcd for  $\text{C}_{10}\text{H}_6\text{N}_2$ : C, 77.90; H, 3.89. Found: C, 77.79; H, 4.08.

**8-Cyanoquinoline Hydrochloride.** The protonated ligand salt was

prepared by dissolving a 1:1 molar ratio of 8-cyanoquinoline and hydrochloric acid in absolute methanol with stirring. The product was slowly precipitated as a white powder by adding a large excess of ether. The compound was collected, washed, and dried in vacuo.

The ligands quinoline and 3-cyanopyridine were obtained from Matheson Coleman and Bell Chemical Co. and Aldrich Chemical Co., respectively. They were used without further purification.

**Dichlorobis(8-cyanoquinoline)palladium(II).** Dichlorobis(benzonitrile)palladium(II)<sup>18</sup> was dissolved in benzene and the ligand was added in excess as a benzene solution. Upon addition of the ligand, the red solution of the starting material immediately turned yellow and produced a yellow precipitate. After refluxing for 1 h, the solvent was decanted and the remaining yellow precipitate was suspended in a chloroform solution of the ligand. The mixture was again refluxed for 1 h before the final product was collected, washed, and dried in vacuo. Anal. Calcd for  $\text{Pd}(\text{C}_{10}\text{H}_6\text{N}_2)_2\text{Cl}_2$ : C, 49.45; H, 2.47. Found: C, 49.36; H, 2.62.

**Dichlorobis(quinoline)palladium(II).** This complex was prepared in a manner analogous to that of the 8-cyanoquinoline complex.

**Dichlorobis(3-cyanopyridine)palladium(II).** Dichlorobis(benzonitrile)palladium(II)<sup>18</sup> was dissolved in benzene and the ligand was added dropwise in excess as a benzene solution. Upon addition of the ligand, the red solution of the starting material turned yellow and produced a yellow precipitate. The precipitate was collected, washed with benzene, and dried in vacuo. Anal. Calcd for  $\text{Pd}(\text{C}_6\text{H}_8\text{N}_4)_2\text{Cl}_2$ : C, 37.37; H, 2.10. Found: C, 37.57; H, 2.67.

**Dichlorobis(8-cyanoquinoline)platinum(II).** A solution of the ligand was prepared by dissolving 0.2 g of 8-cyanoquinoline in 2 ml of ethanol and diluting with water. A 2:1 molar excess of the ligand in solution was added to a hot solution of potassium tetrachloroplatinate in water. With stirring, a yellow precipitate slowly formed which was collected, washed, and dried in vacuo. Anal. Calcd for  $\text{Pt}(\text{C}_{10}\text{H}_6\text{N}_2)_2\text{Cl}_2$ : C, 41.82; H, 2.11. Found: C, 42.01; H, 2.49.

**Dichlorobis(quinoline)platinum(II).** This complex was prepared by heating dichlorodiammineplatinum(II)<sup>19</sup> in quinoline. The dichlorodiammine complex gradually dissolved forming a red-orange solution from which a light yellow precipitate was formed. The product was collected, washed, and dried in vacuo.

**Dichlorobis(8-cyanoquinoline)copper(II).** Hydrated copper(II) chloride was dissolved in triethyl orthoformate to remove the water of hydration. The metal solution was added to a 2:1 excess of the ligand dissolved in triethyl orthoformate. Upon heating, a gray-green precipitate gradually formed which was collected, washed, and dried in vacuo. Anal. Calcd for  $\text{Cu}(\text{C}_{10}\text{H}_6\text{N}_2)_2\text{Cl}_2$ : C, 54.24; H, 2.73. Found: C, 54.26; H, 2.93.

**Dichlorobis(quinoline)copper(II).** This complex was prepared in a manner analogous to that of the 8-cyanoquinoline complex.

**Bis(8-cyanoquinoline)silver Nitrate.** A solution of the ligand was prepared by dissolving 0.2 g of 8-cyanoquinoline in 2 ml of ethanol and diluting with water. An aqueous solution of silver nitrate was